CHAPTER 2

Literature Review

2.1 Definition of Membrane

The membrane can be defined as a solid-phase barrier, that allow preferential passage of certain substances under the influence of a driving force (Singh, 1998). Most membranes are made from the polymeric materials. These materials are light, chemical resistant, cheap and easy to modify the structure to improve the quality of membrane for long term used under demanding applications. The membrane material should be chemically, thermally, and mechanically stable to withstand the separation process environment including the high pressure, temperature and contact with chemical agents.

2.2 Membrane Architecture

The membrane is subdivided into symmetric and asymmetric structures. The symmetric membranes are divided into nonporous and porous.

- Nonporous symmetric membranes are typically made by spreading polymer solution on the glass plate or on a liquid and allowing the solvent to slowly evaporate, such as dense membrane.
- Porous symmetric membranes can be made by radiation bombardment on polymer sheet, followed by leaching. After leaching away the polymer structure damaged by radiation, the result is a membrane with very homogeneous pores.
- Asymmetric membranes, which are more important commercially, come in a wide variety of types. They are made by phase inversion and interfacial polymerization.

Generally, membranes are made by phase inversion process including those in this study. In phase inversion, an asymmetric porous structure is formed when polymer solution is cast on a non woven substrate and immersed in a non solvent bath.

2.3 Formation of Pores by Phase Inversion Method

Controlling the pore size of membrane is important for the separation process of the membranes. The different applications require the membranes with distinct pore ranges. According to the IUPAC classification, pore smaller than 2 nm, required for nanofiltration, are considered as micropores: pores with diameters between 2 and 50 nm, which are characteristic of ultrafiltration membranes, are mesopores, while macropores, useful for microfiltration, are larger than 50 nm (Nunes, 1997)

Phase inversion procedure is commercially more widespread and frequently involves casting the polymer solution onto a suitable non woven material, followed by immersion in a non solvent bath (wet process). In this process, asymmetric porous structure is formed across the membrane film with a selective skin on the surface. The pores occur after immersing in a non-solvent bath due to the solvent exchange method between the solvent and non-solvent. A more open structure beneath the skin enhances the mechanical stability of the membrane (Nunes, 1997). Phase inversion membranes are today widely used in reverse osmosis, nanofiltration, ultrafiltration and microfiltration, and hemodialysis.

Pore formation is driven by phase separation followed by a mobility decrease that freezes a non-equilibrium structure, producing the porous membrane. Phase separation is mainly a liquid-liquid (l-l) demixing process, although solid-liquid (s-l) demixing may also play a role in system containing a crystallizatable polymer. Crystallization is expected to have more influence on pore formation when nuclei are already present in the polymer solution used for casting the membrane.

When a polymer solution is immersed in a non-solvent bath (the usual procedure for membrane preparation) the solvent–non solvent exchange brings the initially thermodynamically stable system into a condition in which a minimum Gibbs free energy is reached with the coexistence of two different phases. The ternary phase (see in Figure 2.1) the binodal curve separates the stable region of the phase diagram from the metastable region; the spinodal is located between the metastable and the unstable region. In the unstable region demixing always spontaneously leads to a decrease in the Gibbs energy whereas in the metastable region an activation energy is required to overcome intermediary states of higher energy and to successfully drive the system into the two-phase condition of lowest energy.

If solvent-nonsolvent exchange leads the membrane-forming film to gel without phase separation, a dense-nonporous film will be formed (Path (a) in Figure 2.1). If a system is brought to a metastable condition, a disperse phase consisting of droplets (nuclei) of a polymer solution with concentration different from that of the matrix tends to be formed. These nuclei must exceed a critical dimension to be stable. This mechanism of l-l phase separation is known as nucleation and growth (NG) (Path (b) in Figure 2.1). During membrane formation, the disperse nuclei are the polymer dilute phase, while the matrix is the polymer concentrated phase. As phase separation proceeds, the size of the nuclei increases (from t_1 to t_2 in Figure 2.1). A low degree of interconnectivity between pores is expected, favoring a membrane with predominantly closed cells. Path (d) in Figure.1 leads to phase separation by NG as well, but in this case, the solution is very dilute. The matrix is the dilute phase, while nuclei are the polymer concentrated phase. No membrane is formed.

When the system is brought from a stable condition to the unstable region, phase separation occurs by spinodal decomposition (SD) (Path (c), Figure 2.1). Because no activation energy is required, fluctuations of composition with continuously increasing amplitude start in the demixing system, giving rise to a regular highly interconnected structure with two continuous phases. As phase separation proceeds (from t_1-t_2, Figure 2.1), the distance between phase increases with the time. Usually membranes with

predominantly interconnected pored can be formed. More important in the initial demixing mechanism is its interruption at a convenient stage and freezing the porous structure by gelation or solidification because if the system does not gel and phase separation can not stop, coalescence may decrease the interconnectivity to the equilibrium condition of complete phase separation shown in the last stages of SD in Figure 2.1c. , (from t_3 to t_4)

During the membrane formation step, first a skin layer is formed beneath the skin, across the whole solution film, demixing may start in conditions that could correspond to different regions of the phase diagram. Therefore different mechanisms may occur in different layers of the membrane film, giving rise to quite asymmetric structures.

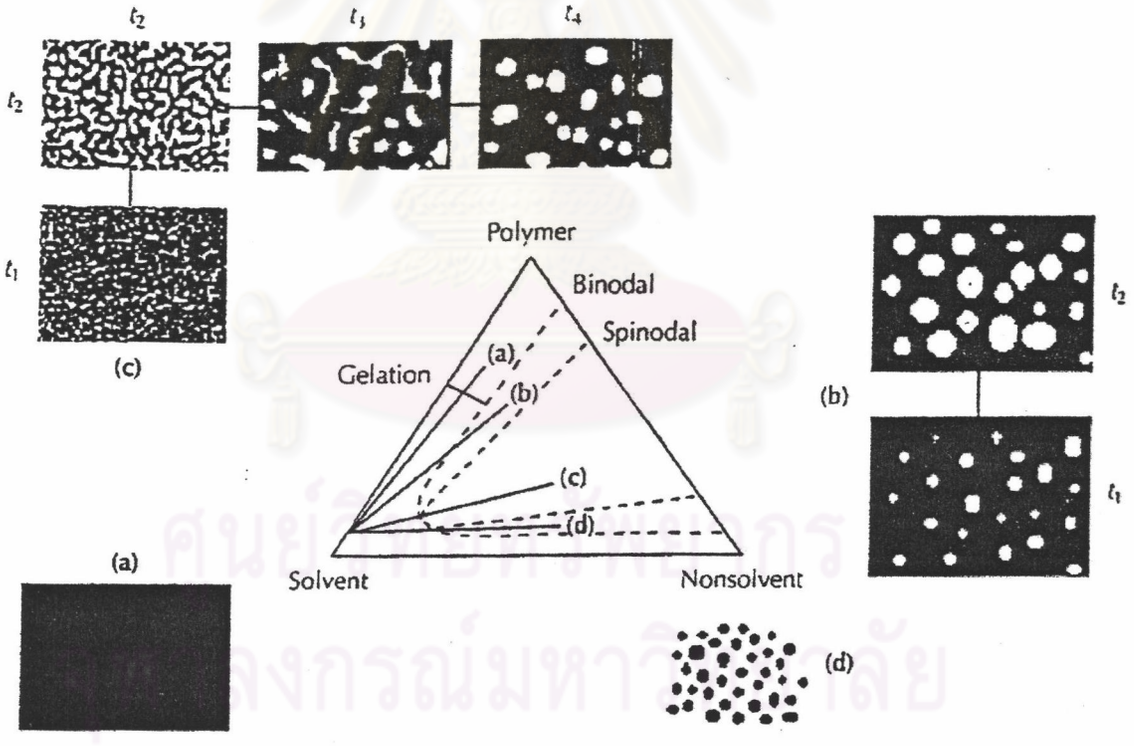

Figure 2.1 Phase separation in ternary systems for membrane preparation (Nunes, 1997)

2.4 Nanofiltration Membrane

2.4.1 Theory

The nanofitration membrane pore size is between those for reverse osmosis and ultrafiltration (average 2 nm.). These membranes have a molecular weight cut off ranges from about 100 to 1000 daltons. Sometimes these membrane are called " loose reverse osmosis" the separation mechanism is sorption-sieving occurred between solute and the membrane surface layer (Singh, 1998).

2.4.2 Introduction of the nanofiltration membrane in the organic solvent recovery.

A nanofiltration membrane acts as barrier to flow allowing selective passage of solvent while other solutes are retained partially or completely under the static temperature and pressure.

Performance of these membranes depends on the molecular weight cut off, defined as the molecular weight of solute for which the membrane shows 90% rejection, controlled by pore size. The solvent flux is determined by solvent-membrane, other solutes-solvent, solute-solvent interactions. These interactions depend on the dielectric constants of solvent and differences amongst the solubility parameters of membrane and solvent. As the organic solvents are usually more hydrophobic than the membrane material, a more hydrophobic membrane would be required to increase the solvent flux. The swelling of membrane in the organic solvents affects the mechanical stability that has implications for a process application. (Musale and Kumar, 2000a,b). The membrane material selection, preparation procedure and structure at the membrane barrier layer (surface morphology) have definite effects on the solvent flux as well.

2.4.3 Other applications of nanofiltration membrane

The nanofiltration membranes are ideally suited for rejecting organics with molecular weights > 200 (e.g. lactose, sucrose, and glucose) and multivalent ions. It will likely replace reverse osmosis for wastewater stream treatment such as desalting cheese whey, removing heavy metals, and separating dyes and color compounds in the textile industry. Nanofitration is superior to both reverse osmosis and ultrafiltration in the treatment of the bleaching effluent from pulp and paper plants. Reverse osmosis is expensive because of the low permeate flux and higher energy cost, and ultrafiltration is ineffective in rejecting low molecular weight chlorinated compounds and in demineralization (Singh, 1998).

2.5 Chitosan

Chitosan, a high molecular weight hydrophilic biopolymer, was prepared by N-deacetylation of chitin with NaOH solution. Chitin is a structural component of crustacean shells and fungal cell wall and obtained at low cost from seafood processing. Chitin is deacetylated about 50% up called as "chitosan".Chitin and chitosan are polysaccharides which at carbon-2 of their cellulose-like backbone have acetamide and amino group; respectively (see in Figure 2.2) (Skjar-Braek, Anthonson and Sandford, 1989). Generally, deacetylation process is rarely complete about 70-90% and N-acetyl groups is about 10-30%, therefore chitosan is a copolymer of N-acetylglucosamine and N-glucosamine repeat units.

Chitosan is soluble in the solvents at pH less than 6.5. The chitosan solution is a cationic polymer as shown in Figure 2.3. These solvents are organic acid such as acetic acid, citric acid and formic acid at 0.2-100 % by volume. In addition, the chitosan could be dissolved in the dilute inorganic acid such as nitric acid.

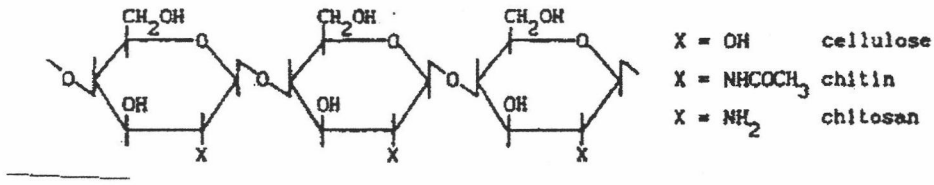

Figure 2.2 Chemical structure of cellulose, chitin, chitosan.
(Skjar-Braek, Anthonson and Sandford, 1989)

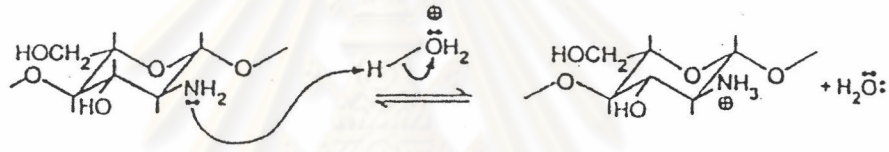

Figure 2.3 The reaction mechanism of chitosan solution
(Skjar-Braek, Anthonson and Sandford, 1989)

Due to its chemical resistance and good mechanical stability, it is used in making ultrafiltration, reverse osmosis, pervaporation membranes. Moreover chitosan's structure has functional groups that are easy to modify. Chitosan is suitable material for the selective layer or surface layer of the composite membranes for above reasons.

The molecular weight of chitosan affected the tensile strength, tensile elongation and permeability. At 90% deacetylated chitosans, the high molecular weight chitosans showed tensile strength and tensile elongation higher than low molecular weight. However, the permeability of membranes prepared from high molecular weight chitosans was lower than those of low molecular weight chitosans (Chen and Hwa, 1996). A higher the chitosan concentration in the dope solution lead to easy aggregation of each chitosan

molecule in the gelation process and denser structure. This results in the higher selectivity and lower permeabilty of membranes. Asymmetric and wholly dense structure were obtained in the cases of NaOH solution and DMSO (dimethylsulfoxide) (Matsuyama, Kitramura and Naramura, 1999)

Chitosan has been used to increase the water permeation separated from ethylene glycol by a chitosan/polysulfone composite pervaporation membrane (Feng and Huang, 1996) and increased the protein transmission by poly(acrylonitrile)/chitosan composite ultrafiltration membrane (Musale and Kumar, 1999).

2.6 Crosslinking Reaction of Chitosan

There were references on crosslinking reaction of the chitosan membrane. The condition of the crosslinked chitosan with glutaraldehyde can be devided into two types: homogeneous and heterogeneous crosslinking.

- Under homogeneous condition, this crosslinking reduces the crystallinity to increase the amount of the accessible chelating groups and hydrophilicity (Koyama and Taniguchi, 1986)

- Under heterogeneous condition used in this research, this crosslinking occurred in the amorphous region, so the adsorption of the water or hydrophilicity reduces with increasing glutaraldehyde concentration (Tual and Espouche, 2000). However, the crosslinker type and size affected membrane performance. The hydrophilic and bulky crosslinker such as sulfosuccinic acid used for the pervaporation separation to increase the flux in dehydration of alcohol solution (Jegal and Lee, 1999). For glutaraldehyde, a hydrophobic crosslinking agent, was suitable for the non polar solvent separation. Musale and Kumar (2000c) showed the structure of crosslinked chitosan by glutaraldehyde (see in Figure 2.4) by Schiff's base formation shown in Figure 2.5 (Morrison and Boyd, 1974)

Chitosan hydrogel membrane became a cationic membrane below its pKa value (pKa value = 6.3), so benzenesulfonic acid (anionic solute) showed the highest permeation, whereas theopylline (cationic solute) showed the lowest although these

solutes have almost the same molecular size. The water flux and permeation of each solutes were almost the same with increasing the glutaraldehyde concentration (Masuyama, Shiraishi and Kitayamura, 1999).

The results showed that more crosslinking reduced the electrostatic effect between membrane and each ionic solutes to separated. Moreover, it also reduced the swelling in the acidic media (Ruckenstein and Zeng, 1996).

Besides, An increase of degree of crosslinking affected higher mechanical strength (Remunan-Lopez and Bodmeier, 1997). Moreover, it also decreased the water content, the solute permeation coefficient and pore radius (Krajewska and Olech, 1996).

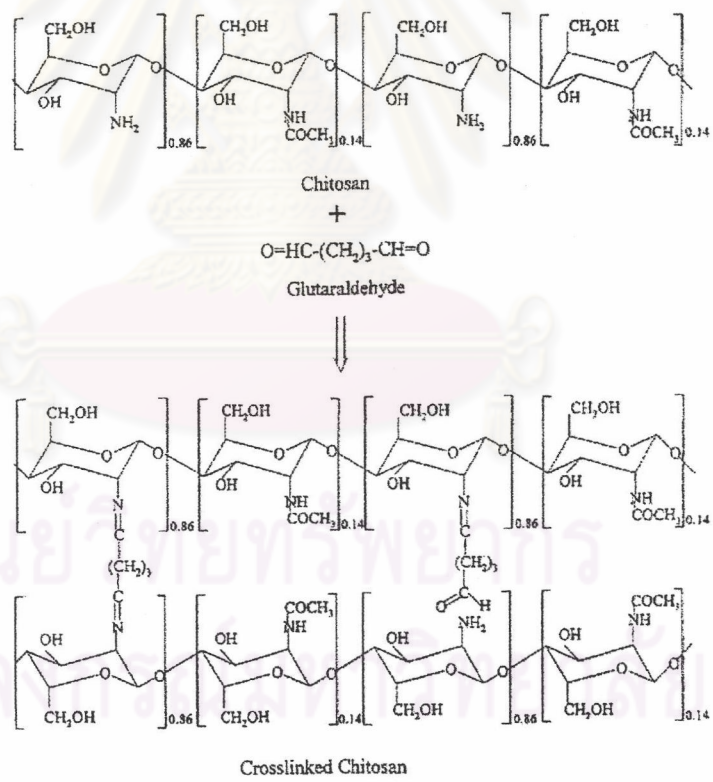

Figure 2.4 Proposed structure for chitosan crosslinked by glutaraldehyde by Schiff's base formation (Musale and Kumar, 2000c)

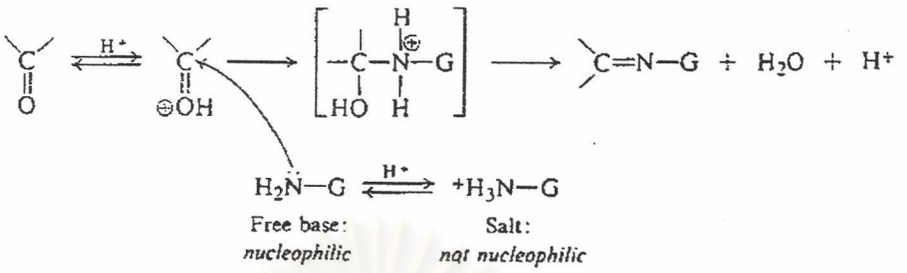

Figure 2.5 Schiff's base formation.(Morrison and Boyd, 1974)

2.7 Determination of Degree of Crosslinking

The degree of crosslinking was determined by using Beer's law or Bouguer-Beer Lambert law (Griffiths and de Haseth, 1986) as shown in equation 2.1 and also the spectral substraction in Fourier Transform Infrared (FT-IR) Spectroscopy.

From equation 2.1,

$$A(\nu) = a(\nu)bc \qquad (2.1)$$

Where, $A(\nu)$ = OD = the absorbance at 1665 cm^{-1}
(imine wavenumber = 1665 cm^{-1})

$a(\nu) = \varepsilon$ = the absorptivity at 1665 cm^{-1} (constant value)

b = l = the pathlength or film thickness (cm.)

c = the imine concentration (equivalent/L)

The adsorptivity of imine groups at 1665 cm^{-1} could be calculated from the slope value of linear curve between the imine absorbance at 1665 cm^{-1} and imine concentration in the standard solution. The standard compound was called as 1,3-di(methylidene)-

cyclohexylamine propane, and its structure (see in Figure 2.6) should be similar to the crosslinked chitosan's.

The solutions were prepared at various concentration to create the linear standard curve between the solution concentration and the imine absorbance at wave number 1665 cm^{-1}. The absorptivity was calculated from slope of this linear curve.

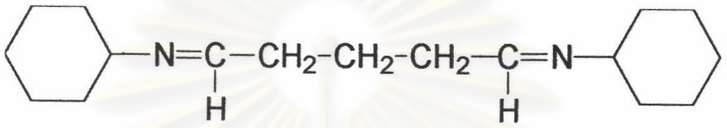

Figure 2.6 The chemical structure of 1,3- di(methylidene)cyclohexylamine propane.

a. Preparation of 1,3- di(methylidene)cyclohexylamine propane

- A 50% w/w aq. glutaraldehyde solution (200 grams) was added to the cyclohexylamine (247.5 grams) drop by drop ($CHO:NH_2$ 1 equivalent:2.5 equivalent), and kept stirring while reacting under N_2 gas and left it overnight covered with parawax film . The product was a yellow, sticky solid and excess cyclohexylamine. This product was dissolved in dichloromethane and separated in the separation funnel .The top layer was aqueous solution with the excess cyclohexylamine and the lower layer was the product dissolved in dichloromethane with trace of the excess cyclohexylamine. The lower solution was put on a petridish , placed in the fume hood overnight and dried in avacuum oven at room temperature for 3 days to remove all dichloromethane and any cyclohexylamine.

The solubilities of this diimine product from cyclohexylamine and glutaraldehyde were tested in the various solvents: distilled water, 95%EtOH, and chloroform. The result is shown in Table 2.1. The product was dissolved in 95% aq.EtOH to give a red solution in a glass tube, then distilled water added drop by drop and shaken at the same time. The

solution started to precipitate and became a cloudy solution. This tube was put into the hot water at about 60°C to re-dissolve the precipitate and then to cool down to the room temperature in the fume hood to let it recrystallize slowly, followed by refrigeration overnight. The crystals of this product appeared at the bottom of tube in the liquid. After decanting the liquid off, the wet product in the tube was placed in vacuum oven at room temperature for 3 days to remove water and ethanol residues.

Table 2.1 Solubility of cyclohexylamine, 50% glutaraldehyde solution and product in each solvents : water, 95%aq. EtOH, chloroform.

Chemical Agents	Solvent		
	Water	95%EtOH	$CHCl_3$
Cyclohexylamine	+	+	+
Glutaraldehyde	+	+	-
Product	-	+	+

\+ : dissolved

\- : not dissolved

b. Preparation the standard solutions at various concentrations of glutaraldehyde/cyclohexylamine product: solutions A,B,C.

Solution A: product (0.0030g.) was dissolved in dichloromethane (5 ml.).

MW_{total} = 262

$MW_{equivalent}$ = 262/2 = 131

[C=N] = (0.003×1000)/(131×5)

= 0.00458 equivalent/L.

Solution B : product (0.0015 g.) was dissolved in dichloromethane (5 ml.) to give a solution , diluted to half the concentration of solution a.

[C=N] = 0.00229 equivalent/L.

Solution C : Mixed the solution b. (1 ml.) with dichloromethane (1 ml.)

[C=N] = 0.001145 equivalent/L.

Each solution was examined by FT-IR to find out the absorbance of imine groups at 1665 cm^{-1} by substraction of the IR spectrum of dichloromethane as shown in Appendix B. The linear standard curve between the absorbance of imine groups and imine concentration in the standard solution was shown in Figure 2.7 to calculate the absorptivity of imine groups.

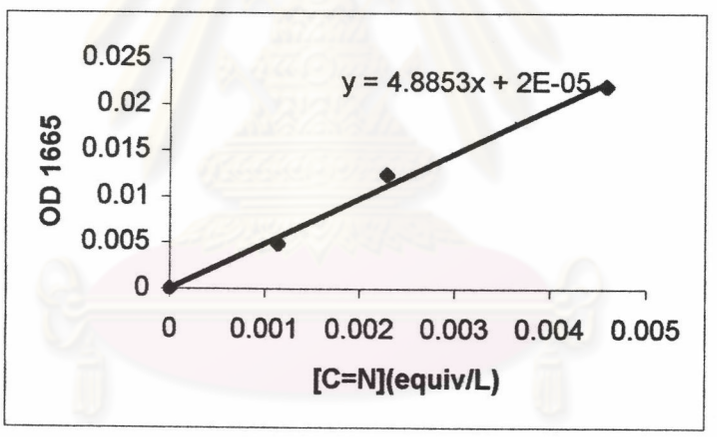

Figure 2.7 Standard curve between the imine concentration ([C=N]) and the imine absorbance at 1665 cm^{-1} (OD 1665)

From equation 2.1)

$$OD = \varepsilon [C=N] l \qquad (2.2)$$

l = the width of the cell or the pathlength (cm.)

= 0.1 cm.

From the linear curve in Figure 2.7,

$$\text{Slope} = 4.9 = 0.1\,\varepsilon$$

Hence; $$\varepsilon = 49\ \text{cm}^{-1}/(\text{equivalent/L.}) \qquad (2.3)$$

Films from each crosslinking condition: (0.02%, 0.04%, 0.06% for 20,40 min) were tested on FT-IR spectroscopy to find out the absorbance of imine groups from each crosslinking condition by substraction of the IR spectrum of uncrosslinked chitosan film. The thickness of films (l) was determined by the micrometer or calculated from factor (f) in the spectral substraction that showed the thickness difference between the crosslinked chitosan and uncrosslinked chitosan.

Computerized spectral substraction leads to different spectral characteristic between the crosslinked chitosan and uncrosslinked chitosan of precisely the same optical thickness.

The thickness of films in each casting was different that resulted in different effective path lengths. Different effective path lengths could be compensated by multiplying the spectrum of uncrosslinked chitosan by a factor f shown in equation 2.4 and substracting the uncrosslinked chitosan scaled from the spectrum of crosslinked chitosan.

$$A_1 - fA_2 = 0 \qquad (2.4)$$

Where, A_1 = the absorbance of the IR spectrum of uncrosslinked chitosan film

A_2 = the absorbance of the IR spectrum of crosslinked chitosan film

f = the scale factor to bring all absorbances bands of crosslinked chitosan to uncrosslinked chitosan

The thickness of crosslinked chitosan films was different from uncrosslinked chitosan films could be calculated by multiplying the thickness of uncrosslinked chitosan films with the f factor shown in equation 2.5.

$$\text{Thickness}_{\text{crosslinked}} = \text{Thickness}_{\text{uncross}} \times f \quad (2.5)$$

$$\text{Thickness}_{\text{uncross}} = 0.0508 \text{ mm. (from micrometer)}$$

Where, $\text{Thickness}_{\text{crosslinked}}$ = The thickness of crosslinked chitosan film (cm.)

$\text{Thickness}_{\text{uncross}}$ = The thickness of uncrosslinked chitosan film (cm.)

The value f from FT-IR of each crosslinking condition was calculated to measure the thickness of each crosslinked chitosan films at different condition. The absorbance of imine groups from substraction, thickness and the absorptivity were substituted in equation 2.2 to determine the imine concentration (equivalent/L) shown in equation 2.6 and crosslinker concentration calculated from equation 2.7. This crosslinker was the non polar =CH-$(CH_2)_3$-CH= link between chitosan chains of crosslinked chitosan films.

$$[C=N] = OD_{1665} / (49) (\text{thickness}_{\text{crosslinked}}) \quad (2.6)$$

$$[\text{crosslinker}] = [C=N]/2 \quad (2.7)$$

2.8 Membrane Testing.

Membrane Testing was referred from National Research Council Report on membrane fabrication and testing manual. Membrane Testing involved test equipment.

1. Test Equipment

Schematic diagrams of the ultrafiltration test systems with twelve cells arranged in four parallel banks of three cells as long as adequate feed flows were

maintained shown in Figure 2.8. All experiments were carried out with the apparatus shown in Figure 2.9. Each cells was designed as a radial flow pattern, with the feed inlet from the center or the annular perimeter of the cell. The membrane (active area 1.4×10^{-3} m^2) was mounted upside down to prevent suspended matter from settling on the membrane surface during periods of operation where the feed flow is reduced. The gap was spacing between the membrane and the cell body control the velocity of the solution across the membrane surface and the flow pattern created controls the concentration gradients in the vicinity of the membrane surface. The design of cell was shown in Figure 2.10 and test cell (see in Figure 2.11)

The test solute or water was filtered and pumped up to each cells bypass value, and the feed rate to test cells could be varied by using a fixed speed pump and bypass value. The pressure gauges are used to measure the pressure at the inlet and outlet of the test cells. For ultrafiltration system, the operating pressure was about 10-100 psig, but this study, the pressure was controlled at 50 psig. The feed flow can be measured by the a rotameter or the flow rate obtained by measuring the weight or the volume of circulating feed solution collected during a given period of time. Permeate flow rates (F; $L.m^{-2}.h^{-1}$or $g.m^{-2}.h^{-1}$) are best measured by weighing a sample or volume collected during a known period.

$$F = W/At \qquad (2.8)$$

Where; W = the total volume (l.) or weight (g.) of the water or solution permeated during the experiment.

A = the membrane area (m^2)

t = the operation time (hour)

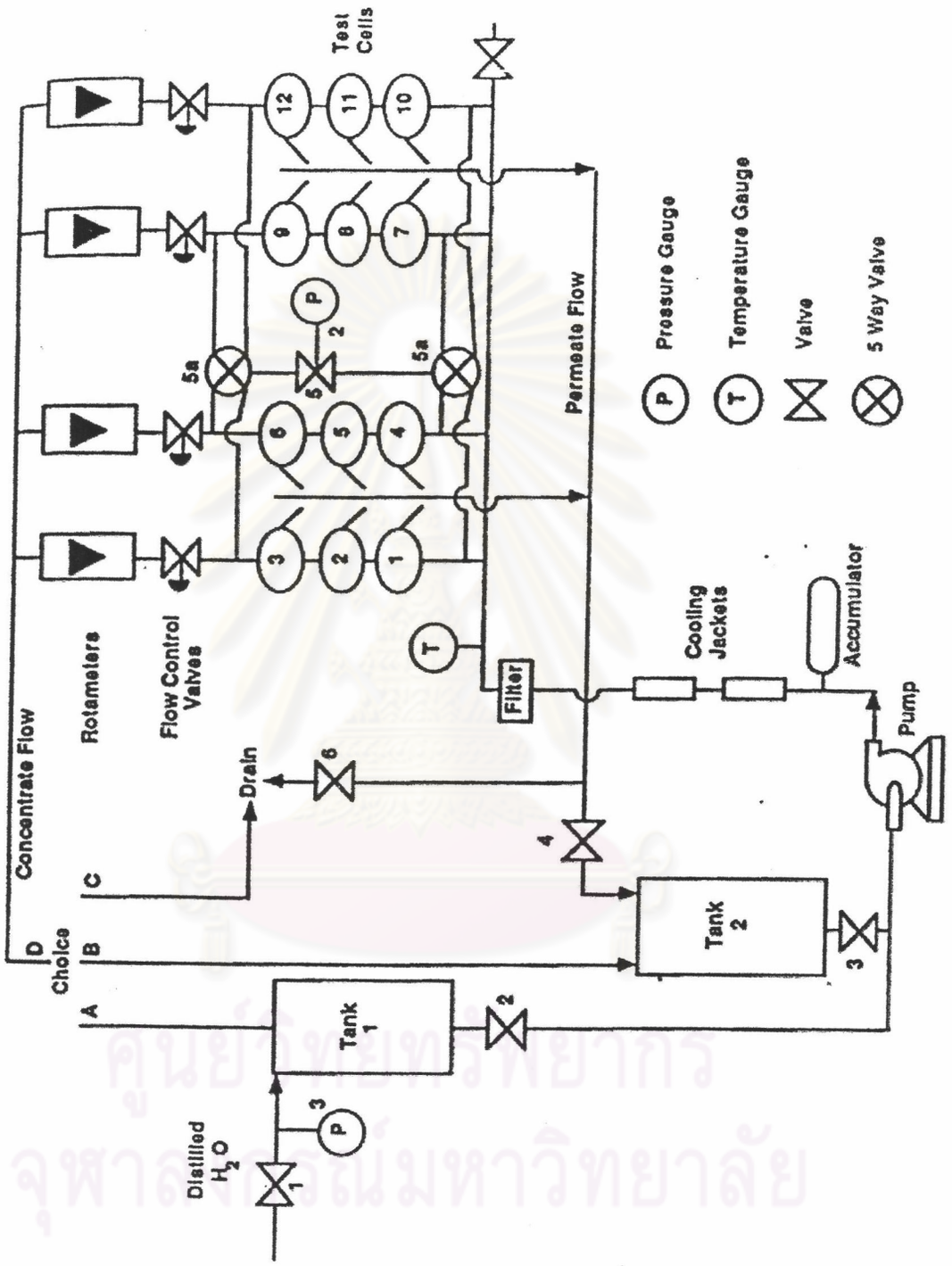

Figure 2.8 Schematic diagram of ultrafiltration membrane test apparatus (Tweddle and Striez, 1994)

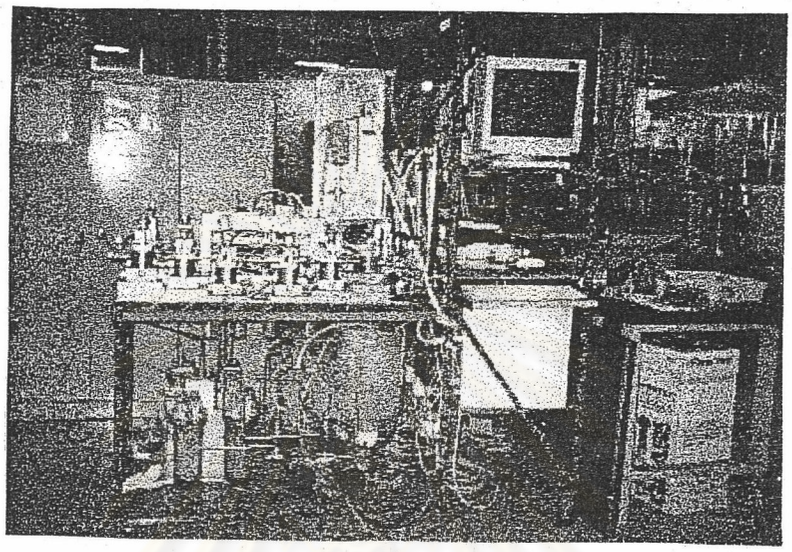

Figure 2.9 Test apparatus

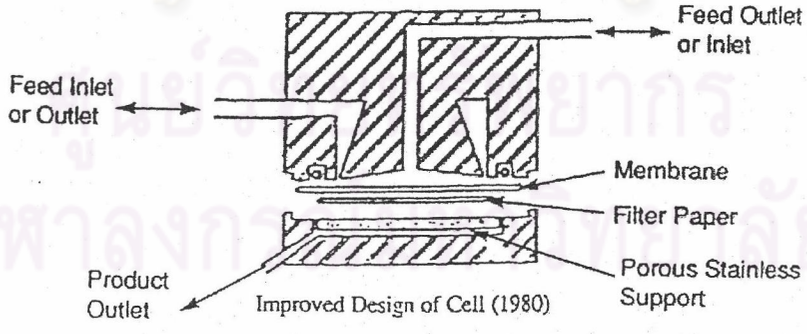

Figure 2.10 Design of test Cell. (Tweddle and Striez, 1994)

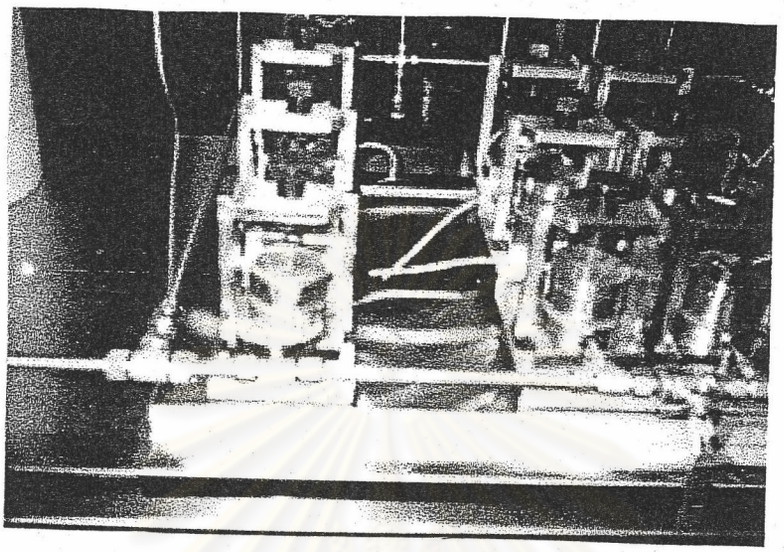

Figure 2.11 Test cell.

Tests are normally run at room temperature (25°C) which was measured by dial thermometer. Each solutes of various molecular weight was dissolved in the plastic bottle 250 ml. and diluted in the water tank until the concentration about 200 ppm. The solutes pass through every membrane in each cell under the constant pressure and flow rate during a known period. The obtained permeate was analyzed with TOC to know the percentage of separation of membrane.

2.9 Percentage of Separation

The percentage of separation of membrane was calculated from equation 2.9.

$$\% \text{ Separation} = \frac{(\text{feed}) - (\text{permeate})}{(\text{feed})} \times 100\% \qquad (2.9)$$

Where ; feed = concentration of feed solute (ppm.)
= 200 ppm.
permeate = concentration of permeate solute obtained from TOC (ppm.)

In principle, Total Carbon (TC) combustion tube was filled with Pt catalyst obtained from Shimadzu Corp. , and heated to 680°C. When sample had been introduced by a sample injection into the TC combustion tube (100µl at the maximum for TC catalyst), TC component in the sample combusted or decomposed to become CO_2. It was then sent through a halogen scrubber into a sample cell set in a non-dispersive infrared gas analyzer where CO_2 is detected. The NDIR outputs a detection signal (analog signal) which generated a peak whose area was calculated by a data processor.

The peak area was proportional to the TC concentration of the sample. Therefore, if calibration curve equation expressing the relation between peak area and TC concentration had been obtained in advance using TC standard solution. The standard solution used was polyethylene glycol solution at various concentration to make a standard curve. The TC concentration of the sample could be determined from the calculated peak area. As preparing standard solution, TC in pure water process affected the TC content in the standard solution. In order to make measurement error minimized, equation 2.9 must be corrected by TC concentration of pure water as shown in the following equation 2.10:

$$\% \text{ Separation} = \frac{(\text{feed} - TC_{\text{pure water}}) - (\text{permeate} - TC_{\text{pure water}})}{(\text{feed} - TC_{\text{pure water}})} \times 100\% \qquad (2.10)$$

Where ; feed = concentration of feed solute (ppm.)
= 200 ppm.
Permeate = concentration of permeate solute obtained from TOC (ppm.)
$TC_{\text{pure water}}$ = TC concentration of pure water (ppm.)

This TC value was used in the calculation of % separation of membrane, then lead to the molecular weight cut off (MWCO) of membrane.

2.10 Background of Surface Crosslinked Chitosan/Poly(acrylonitrile) Composite Nanofiltration Membranes in the Organic Solvent Recovery.

Since the commercial nanofiltration membrane could not withstand the organic solvent for long operation time and also low solvent flux, therefore nanofiltration composite membrane are composed of three layers: selective dense layer, porous substrate layer (ultrafiltration membranes) and backing material (non-woven fabric). Ultrafiltration (UF) membranes are used for supporting selective thin layers and sometimes can have definite resistance for permeation. A thin-film composite structure in which a thin skin (dense membrane) at the top facing the feed solution acts as the selective layer. The pressure drop in the porous backing of such membrane is usually very small; further this packing has almost no influence on the solute rejection properties of the membrane. Transport and rejection models focus only on the thin membrane skin or surface layer (see in Figure 2.12) provides a schematic of such a membrane structure. Therefore the solute rejection or solvent flux depend on type and structure of the selective layer and selective layer/solute interaction (Sirkar and Winston, 1992).

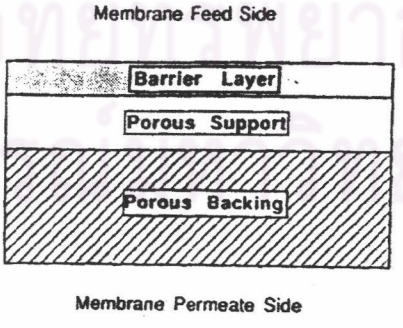

Figure 2.12 Thin-film composite membrane structure (Sirkar and Winston, 1992).

The crosslinked chitosan was more hydrophobic with increasing glutaraldehyde concentration and crosslinking time to increase the solvent affinity. Musale and Kumar (2000b) made the nanofiltration composite membrane which are composed of three layers: backing material (nonwoven polyester), porous substrate layer (polyacrylonitrile ultrafiltration membranes) and the selective layer was glutaraldehyde crosslinked chitosan layer. The crosslinked chitosan was more hydrophobic with increasing glutaraldehyde concentration and crosslinking time to increase the non-polar solvent affinity.

Relation between permeation, diffusion and swelling of membrane in solvent explained in Fickian mechanism as follows in equation 2.11;

$$P = DS \qquad (2.11)$$

Where, P = Permeation coefficient

D = Diffusion coefficient

S = The sorption coefficient , which is ratio of the mass of the solvent sorbed to that of the initial weight of polymer.

Musale and Kumar (2000b) concluded about the resistance of surface crosslinked chitosan/poly(acrylonitrile) composite nanofiltration membrane to pH and organic solvents with increasing the glutaraldehyde concentration or crosslinking time. The permeation of aqueous acidic (pH 2.5) and basic (pH 11) solution as well as pH range of 2.5-11. After increased crosslinking of chitosan surface layer, this membrane maintained the higher permeate fluxes for test solvents with increasing glutaraldehyde concentration for two hours.

The solvent flux increased after crosslinking may be due to an increase in hydrophobicity of membrane, caused by insertion of nonpolar $=CH-(CH_2)_3-CH=$ links between chitosan chains, resulting in increased affinity with organic solvents.

The swelling of polar alcohol (ε = 18.3-32.6)> MEK (ε = 15.4) > EtOAc (ε = 6.02)> Hexane (ε = 1.9) that swelling clearly relate to dielectric constant (ε) of solvent at the same crosslinking condition as the higher dielectric constant of solvent affected the lower solvent flux decreased. This result could be explained by the membrane-solvent polar reaction and the difference of solubility parameters between chitosan membrane and solvent ($\delta_{chitosan} - \delta_{solvent}$). After the solvent flux test, the polar solvents such as polar alcohol destroyed the NF membrane as shown by SEM, but there was no evidence from destruction of non polar solvent on NF membrane (Musale and Kumar, 2000b).

The higher degree of crosslinking usually results in an increase in mechanical strength. However, at a very high degree of crosslinking, chitosan membranes became weaker due to increased brittle surface (Remunan-Lopaz and Bodmeier, 1997). The cause of the composite nanofiltration membrane maintained the higher solvent flux only 2 hours. This result might be assumed that the chitosan layer was damaged because the degree of crosslinking was too high that the chitosan layer became weak.